Temperature affects the morphology and calcification of Emiliania huxleyi strains

Article *in* Biogeosciences · May 2016

DOI: 10.5194/bg-13-2913-2016

3 authors, including:

Anaid Rosas Navarro
Autonomous University of Barcelona
4 PUBLICATIONS **3** CITATIONS
SEE PROFILE

Patrizia Ziveri
Catalan Institution for Research and Advance…
153 PUBLICATIONS **3,553** CITATIONS
SEE PROFILE

Biogeosciences, 13, 2913–2926, 2016
www.biogeosciences.net/13/2913/2016/
doi:10.5194/bg-13-2913-2016

Biogeosciences Open Access EGU

Temperature affects the morphology and calcification of *Emiliania huxleyi* strains

Anaid Rosas-Navarro[1], Gerald Langer[2], and Patrizia Ziveri[1,3]

[1]Institute of Environmental Science and Technology (ICTA), Autonomous University of Barcelona (UAB), 08193 Bellaterra, Spain
[2]The Marine Biological Association of the United Kingdom, The Laboratory, Citadel Hill, Plymouth, Devon, PL1 2PB, UK
[3]Catalan Institution for Research and Advanced Studies (ICREA), 08010 Barcelona, Spain

Correspondence to: Anaid Rosas-Navarro (anaid.rosas@uab.cat), Gerald Langer (gerlan@MBA.ac.uk), and Patrizia Ziveri (patrizia.ziveri@uab.cat)

Received: 22 November 2015 – Published in Biogeosciences Discuss.: 18 January 2016
Revised: 26 April 2016 – Accepted: 26 April 2016 – Published: 18 May 2016

Abstract. The global warming debate has sparked an unprecedented interest in temperature effects on coccolithophores. The calcification response to temperature changes reported in the literature, however, is ambiguous. The two main sources of this ambiguity are putatively differences in experimental setup and strain specificity. In this study we therefore compare three strains isolated in the North Pacific under identical experimental conditions. Three strains of *Emiliania huxleyi* type A were grown under non-limiting nutrient and light conditions, at 10, 15, 20 and 25 °C. All three strains displayed similar growth rate versus temperature relationships, with an optimum at 20–25 °C. Elemental production (particulate inorganic carbon (PIC), particulate organic carbon (POC), total particulate nitrogen (TPN)), coccolith mass, coccolith size, and width of the tube element cycle were positively correlated with temperature over the sub-optimum to optimum temperature range. The correlation between PIC production and coccolith mass/size supports the notion that coccolith mass can be used as a proxy for PIC production in sediment samples. Increasing PIC production was significantly positively correlated with the percentage of incomplete coccoliths in one strain only. Generally, coccoliths were heavier when PIC production was higher. This shows that incompleteness of coccoliths is not due to time shortage at high PIC production. Sub-optimal growth temperatures lead to an increase in the percentage of malformed coccoliths in a strain-specific fashion. Since in total only six strains have been tested thus far, it is presently difficult to say whether sub-optimal temperature is an important factor causing malformations in the field. The most important parameter in biogeochemical terms, the PIC : POC ratio, shows a minimum at optimum growth temperature in all investigated strains. This clarifies the ambiguous picture featuring in the literature, i.e. discrepancies between PIC : POC–temperature relationships reported in different studies using different strains and different experimental setups. In summary, global warming might cause a decline in coccolithophore's PIC contribution to the rain ratio, as well as improved fitness in some genotypes due to fewer coccolith malformations.

1 Introduction

Emiliania huxleyi (Lohmann) Hay and Mohler is a cosmopolitan (McIntyre and Bé, 1967; Brown, 1995), genetically diverse (Medlin et al., 1996; Schroeder et al., 2005; Iglesias-Rodríguez et al., 2006; Hagino et al., 2011; Read et al., 2013), morphologically variable (Hagino et al., 2005; Hagino and Okada, 2006; Cubillos et al., 2007) marine photosynthetic and calcifying (Brownlee and Taylor, 2004) unicellular haptophyte algae species and the most abundant of the coccolithophores. It produces calcite ($CaCO_3$) plates called coccoliths which cover the cell. As a photosynthetic organism, *E. huxleyi* shifts the seawater carbonate system towards [CO_3^{2-}], but as a calcifier it shifts the seawater carbonate system towards [CO_2]. Therefore, part of the interest in *E. huxleyi* derives from its role in the global carbon cycle. In particular, extensive blooms (Westbroek et al., 1993;

Paasche, 2001) might impact air–sea gas exchange (Robertson et al., 1994; Buitenhuis et al., 1996). Climate-change-induced surface water stratification was shown to trigger *E. huxleyi* blooms (Harada et al., 2012).

The ratio of particulate inorganic carbon (PIC) and particulate organic carbon (POC) influences surface water–atmosphere gas exchange as well as the composition of matter exported from surface waters to the deep ocean (Ridgwell and Zeebe, 2005; Findlay et al., 2011). The response of PIC and POC production and their ratio in the prolific species *E. huxleyi* to temperature is a necessary first step towards an understanding of its possible impact on global biogeochemical cycles.

The relationship of PIC production/PIC : POC and temperature in *E. huxleyi* is not clear. De Bodt et al. (2010) found that PIC production was higher at lower temperatures in a strain grown at 13 and 18 °C, while Sett et al. (2014) found the opposite in another strain grown at 10, 15 and 20 °C. De Bodt et al. (2010) found higher PIC : POC ratios at lower temperatures for a strain of *E. huxleyi* and Gerecht et al. (2014) found a similar relationship for a strain of the species *Coccolithus pelagicus*. Sett et al. (2014), however, found a different relationship for the PIC : POC ratio in another strain of *E. huxleyi*, which is not supported by the experiment of Langer et al. (2007) on the same strain. Feng et al. (2008) did not find differences in the PIC : POC ratio in another strain grown at 20 and 24 °C. These discrepancies between studies might stem from different experimental setups and a lack of knowledge of the optimum growth temperature or indeed strain-specific differences (Hoppe et al., 2011). Therefore, it is necessary to test more than one strain for its temperature response under otherwise identical conditions. This we have done in the present study.

Apart from biogeochemical considerations, global warming might also be of interest in terms of the ecological success of coccolithophores, because different groups of organisms might be differently affected by warming and therefore ecological succession patterns, grazing pressure etc. might change. The latter was proposed to depend on coccolith morphology more than it does on PIC production (Langer et al., 2011). The effect of temperature on coccolith morphogenesis is evident in field observations (Bollmann, 1997; Ziveri et al., 2004) and is best assessed with respect to the optimum growth temperature in laboratory experiments. While the effect of supra-optimal temperature is unequivocally detrimental (Watabe and Wilbur, 1966; Langer et al., 2010), it is not clear whether there is an effect of sub-optimal temperature at all (Watabe and Wilbur, 1966; Langer et al., 2010; De Bodt et al., 2010). A temperature increase in the sub-optimal range is probably what most coccolithophore clones will experience in the course of global warming (this study Buitenhuis et al., 2008; Langer et al., 2009; Heinle, 2014), and therefore this temperature range is particularly interesting. In the present study we focus on coccolith morphology under sub-optimal temperature, doubling the amount of data currently available, and thereby clarifying whether sub-optimal temperatures can cause malformations. We selected three strains of *E. huxleyi* from a single area, the Japanese coast in the North Pacific Ocean, in order to assess the plasticity within strains originating from a particular environmental setting.

2 Materials and methods

2.1 Pre-culture and batch culture experiments

Clonal cultures of *Emiliania huxleyi* were obtained from the Roscoff Culture Collection. We selected three strains of *E. huxleyi*, two from the Japanese coast in the North Pacific Ocean (RCC1710 – synonym of NG1 and RCC1252 – synonym of AC678 and MT0610E) and a third strain from the same region but of unknown exact origin and strain name, named here IAN01. Strain RCC1710 was collected off Nagasaki at Tsushima Strait (Japan) and RCC1252 at Tsugaru Strait (Japan); both places are strongly influenced by the Tsushima warm current. Additional information about the strain RCC1252 can be found at http://roscoff-culture-collection.org/.

The culture media was sterile-filtered North Sea water (filtered through 0.2 µm pore size sterile Sartobran 300 filter cartridges, Sartorius, Germany) supplemented with nutrients (nitrate and phosphate), metals and vitamins according to Guillard and Ryther (1962). Cell densities were determined using a Multisizer 3 Coulter Counter (Beckman Coulter for particle characterization). To prevent significant changes in seawater carbonate chemistry, maximum cell densities were limited to $\approx 1\times10^5$ cells mL^{-1} (e.g. Oviedo et al., 2014). We used a 16/8 light/dark cycle, and an irradiance of ≈ 300 µmol photons s^{-1} m^{-2}. The three strains were grown for at least 20 generations.

The dilute batch culture experiments were conducted in triplicate, for the strains RCC1710 and RCC1252 at 10, 15, 20 and 25 °C of temperature, and for IAN01 at 15, 20 and 25 °C. The strains were grown in 2 L of sea water within transparent sterilized 2.3 L glass bottles. Cell density at inoculation was 500 to 1000 cells mL^{-1}, and at harvest it was a maximum of 1×10^5cells mL^{-1}. Harvesting was done 9 h after the onset of the light period.

Growth rate was calculated from exponential regression according to

$$\mu = (\ln c_1 - \ln c_0)\,\Delta t^{-1}, \quad (1)$$

where c_1 and c_0 are the final cell concentration and the initial cell concentration, respectively, and Δt is the duration of incubation in days. Averages of triplicates and SD were used in tables and figures (Table 1 and Fig. 1a).

2.2 Carbonate chemistry

The seawater carbonate system was monitored because temperature and coccolithophore production alter the system. We

Table 1. Growth rate and cellular PIC, POC, and TPN content and production of the three strains of *E. huxleyi* at different temperatures. Standard deviation of the triplicates in parentheses. Measured growth rates for extra temperatures from the pre-experiments are included, but PIC, POC and TPN were not measured for these temperatures.

Strain	T (°C)	Growth rate (μ)	PIC (pg cell^{-1})	POC (pg cell^{-1})	TPN (pg cell^{-1})	P_{PIC} (pg cell^{-1} d^{-1})	P_{POC} (pg cell^{-1} d^{-1})	P_{TPN} (pg cell^{-1} d^{-1})
RCC1710	6.5	0.19						
RCC1710	10	0.26 (0.00)	15.31 (0.15)	8.91 (0.29)	1.54 (0.07)	3.98 (0.03)	2.32 (0.08)	0.40 (0.01)
RCC1710	15	0.75 (0.01)	14.07 (0.40)	9.90 (0.11)	1.47 (0.01)	10.55 (0.41)	7.42 (0.16)	1.10 (0.01)
RCC1710	20	1.15 (0.02)	11.47 (0.09)	12.05 (0.79)	1.71 (0.06)	13.16 (0.15)	13.82 (0.63)	1.98 (0.04)
RCC1710	25	1.24 (0.01)	10.80 (0.24)	9.30 (0.80)	1.38 (0.04)	13.34 (0.33)	11.48 (0.99)	1.70 (0.06)
RCC1710	27.5	1.04						
RCC1710	30	0.23						
RCC1252	6.5	0.18						
RCC1252	10	0.26 (0.04)	8.29 (0.49)	6.35 (0.11)	1.16 (0.03)	2.15 (0.39)	1.64 (0.23)	0.30 (0.04)
RCC1252	15	0.73 (0.00)	9.92 (0.32)	8.64 (0.29)	1.34 (0.03)	7.22 (0.23)	6.29 (0.22)	0.97 (0.02)
RCC1252	20	1.15 (0.14)	9.89 (0.28)	8.75 (0.71)	1.35 (0.07)	12.01 (0.74)	9.99 (1.13)	1.56 (0.26)
RCC1252	25	1.22 (0.02)	12.20 (0.21)	10.19 (0.75)	1.41 (0.02)	14.84 (0.38)	12.39 (0.86)	1.72 (0.02)
RCC1252	27.5	1.02						
RCC1252	30	0.00						
IAN01	6.5	0.12						
IAN01	15	0.81 (0.01)	10.18 (0.30)	9.89 (0.43)	1.47 (0.08)	8.20 (0.19)	7.97 (0.30)	1.18 (0.06)
IAN01	20	1.17 (0.00)	8.12 (0.21)	8.95 (0.43)	1.75 (0.09)	9.46 (0.25)	10.43 (0.51)	2.04 (0.11)
IAN01	25	1.32 (0.03)	11.21 (0.36)	9.95 (0.11)	1.46 (0.01)	14.84 (0.49)	13.17 (0.22)	1.94 (0.03)
IAN01	27.5	1.01						
IAN01	30	−0.11						

employed the dilute batch method (Langer et al., 2013) to minimize production effects.

During the harvesting, samples for total alkalinity (TA) measurements were sterile-filtered (0.2 µm pore size) and stored for less than 2 months prior to measurement in 25 mL borosilicate flasks at 4 °C. TA was calculated from linear Gran plots (Gran, 1952) after potentiometric titration (in duplicate) (Bradshaw et al., 1981; Brewer et al., 1986).

Samples for dissolved inorganic carbon (DIC) were sterile-filtered (0.2 µm pore size) with gentle pressure using cellulose-acetate syringe filters and stored bubble-free for less than 2 months prior to measurement at 4 °C in 5 mL borosilicate flasks. DIC was measured, in triplicate, using a Shimadzu TOC 5050A.

The carbonate system was calculated from temperature, salinity (32 ‰), TA and DIC, using the program CO2SYS (Lewis and Wallace, 1998), applying the equilibrium constants from Mehrbach et al. (1973), refitted by Dickson and Millero (1987). For an overview of carbonate chemistry final conditions in all treatments, see Table 2.

2.3 Particulate organic and inorganic carbon, particulate nitrogen and calcite

Duplicate samples for the determination of total particulate carbon (TPC) and total particulate nitrogen (TPN) were filtered onto pre-combusted (500 °C; 12 h) 0.6 µm nominal pore size glass fibre filters (Whatman GF/F), placed in pre-combusted Petri dishes (500 °C; 12 h), oven-dried (60 °C 24 h) and stored at −20 °C. Before analysis, TPC and TPN samples were dried for 24 h in a drying cabinet at 60 °C prior to measurement. All samples were then measured on a Euro EA analyser (Euro Vector).

Particulate inorganic carbon (PIC) was calculated measuring calcium content of samples with 3.6×10^6 *E. huxleyi* cells filtered onto 47 mm polycarbonate (PC) filters (0.8 µm pore size). PC filters were immersed overnight in an acid solution of 1 % HNO_3 to dissolve calcite. Calcium was determined by analysing an aliquot of the samples using an inductively coupled plasma mass spectrometer (ICP-MS, Agilent model 7500ce). Cellular PIC was calculated from the molecular mass of calcite, using the following equations:

$$\mathrm{PIC}_{\mathrm{cell}^{-1}} = \frac{\mathrm{PIC_s}}{c \cdot V_s}, \quad \text{where} \quad \mathrm{PIC_s} = \frac{[\mathrm{Ca}^{2+}]_s \cdot 12.0107}{40.078}, \qquad (2)$$

where $\mathrm{PIC}_{\mathrm{cell}^{-1}}$ is the cellular PIC (in pg), $\mathrm{PIC_s}$ is the PIC sampled contained in the filter (in pg), c is the cell concentration (in cells L^{-1}), V_s is the volume sampled (in L), $[\mathrm{Ca}^{2+}]_s$ is the calcium content in the sample (in pg), 12.0107 corresponds to the relative atomic mass of carbon, and 40.078 corresponds to the relative atomic mass of calcium. Particulate organic carbon (POC) was calculated as the difference between TPC and PIC. PIC, POC and TPN production (P_{PIC}, P_{POC}, P_{TPN}) were estimated as the product of cellular PIC,

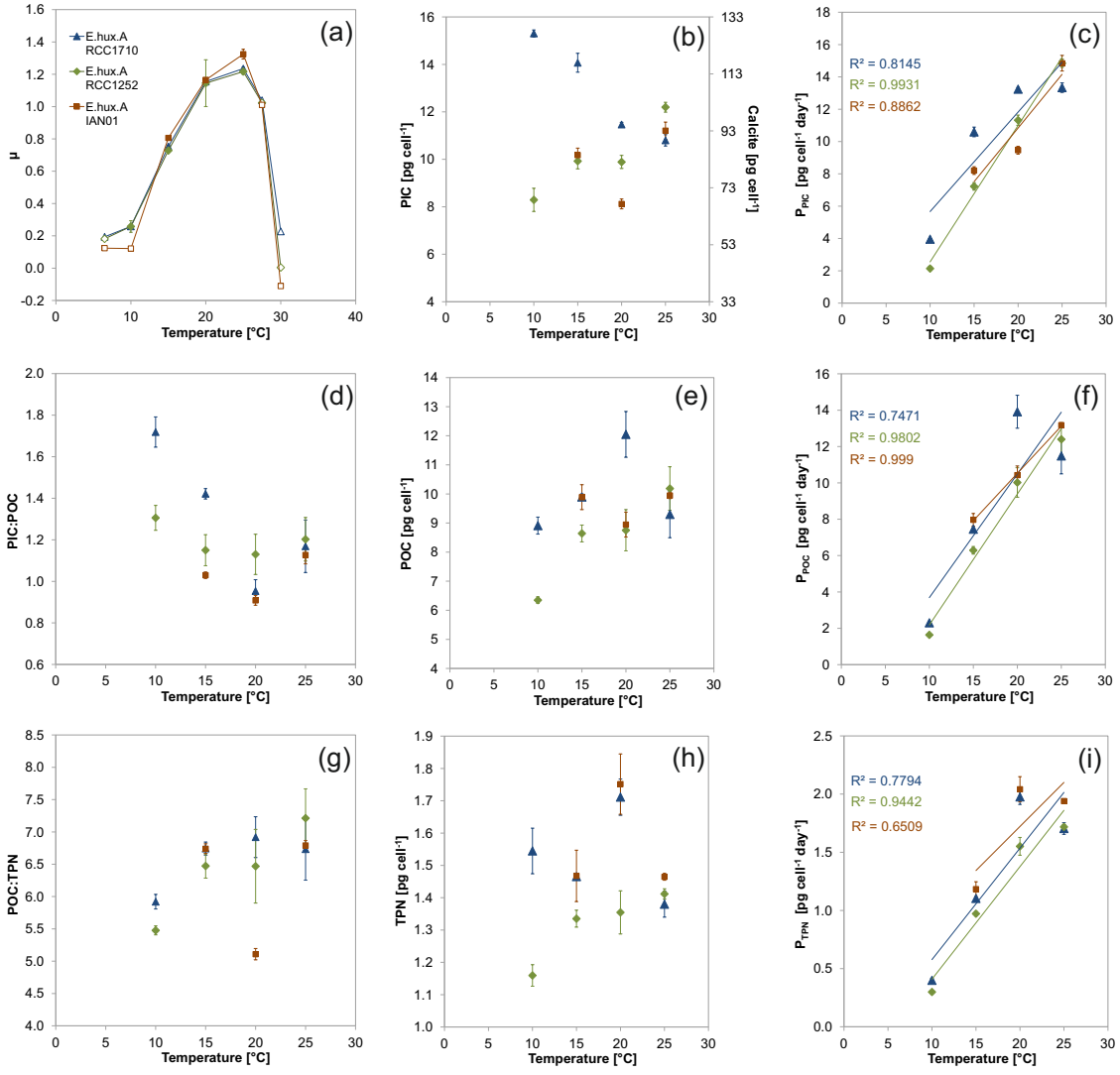

Figure 1. Results at different temperatures. Growth rate **(a)** (extra temperatures from pre-experiments are included and shown as empty symbols); cellular PIC and its concomitant calcite **(b)**, POC **(e)** and TPN **(h)** content; PIC **(c)**, POC **(e)** and TPN **(i)** production (linear trend lines and *r* squared values are shown); and PIC : POC ratio **(d)** and POC : TPN ratio **(g)**. Standard deviations of the triplicate experiment results are shown. Three different strains of *E. huxleyi* were used.

POC or TPN, and growth rate. Calcite ($CaCO_3$) per cell (concomitant of PIC) can also be estimated, substituting in Eq. (2) the calcium carbonate molecular mass (100.0869) in place of the relative atomic mass of carbon. The ratio between PIC and POC (PIC : POC) and the ratio between POC and TPN (POC : TPN) were also calculated.

2.4 Coccolith morphology – by scanning electron microscopy

Thirty millilitres of culture was filtered onto polycarbonate filters (0.8 µm pore size) and dried at 60 °C for 24 h. A small portion ($\sim 0.7\,cm^2$) of each filter was mounted on an aluminium stub and coated with gold (EMITECH K550X sputter coater). Images were captured along random transects using a ZEISS-EVO MA10 scanning electron microscope (SEM).

Emiliania huxleyi SEM images were used to measure and categorize 300 coccoliths per sample (e.g. Langer et al., 2009); the coccoliths were on coccospheres. The tube width (width of the tube elements cycle) of each coccolith (Fig. 2c) was the average of the tube width measured on the two semi-minor axes (along the coccolith width) on the distal view of the coccolith. Tube width measurements were manually taken using the program Gimp-2.8. Examples of the tube width variations in the three different strains are shown in Fig. 2. The 300 coccoliths were classified as normal, malformed or incomplete (e.g. Langer et al., 2011), as described in Table 3, with examples in Figs. 3 and 4.

Table 2. The carbonate system final values. Standard deviation of the triplicates in parentheses.

Strain	T (°C)	TA ($\mu mol\,kg^{-1}$)	DIC ($\mu mol\,kg^{-1}$)	pH (total scale)	pCO_2 (μatm)	HCO_3^- ($\mu mol\,kg^{-1}$)	CO_3^{2-} ($\mu mol\,kg^{-1}$)	Omega calcite
RCC1710	10	2138 (23)	2012 (3)	7.95 (0.07)	482 (74)	1893 (14)	98 (15)	2.38 (0.36)
RCC1710	15	2167 (14)	2023 (12)	7.92 (0.01)	530 (13)	1893 (11)	111 (3)	2.69 (0.07)
RCC1710	20	2291 (25)	2110 (4)	7.92 (0.06)	571 (84)	1953 (19)	139 (18)	3.39 (0.45)
RCC1710	25	2306 (24)	2123 (7)	7.86 (0.03)	688 (55)	1961 (4)	142 (11)	3.51 (0.28)
RCC1252	10	2249 (8)	2095 (12)	8.02 (0.03)	427 (30)	1959 (16)	117 (6)	2.84 (0.15)
RCC1252	15	2219 (57)	2065 (6)	7.94 (0.12)	533 (136)	1925 (21)	119 (32)	2.90 (0.78)
RCC1252	20	2212 (20)	2043 (15)	7.91 (0.01)	571 (10)	1896 (11)	129 (4)	3.15 (0.09)
RCC1252	25	2229 (8)	2052 (10)	7.85 (0.04)	670 (64)	1896 (19)	137 (11)	3.37 (0.26)
IAN01	15	2206 (9)	2064 (16)	7.92 (0.02)	551 (33)	1932 (19)	111 (4)	2.70 (0.11)
IAN01	20	2249 (28)	2106 (6)	7.84 (0.05)	698 (86)	1969 (5)	115 (14)	2.80 (0.34)
IAN01	25	2243 (2)	2066 (4)	7.85 (0.01)	677 (13)	1910 (5)	137 (2)	3.37 (0.05)

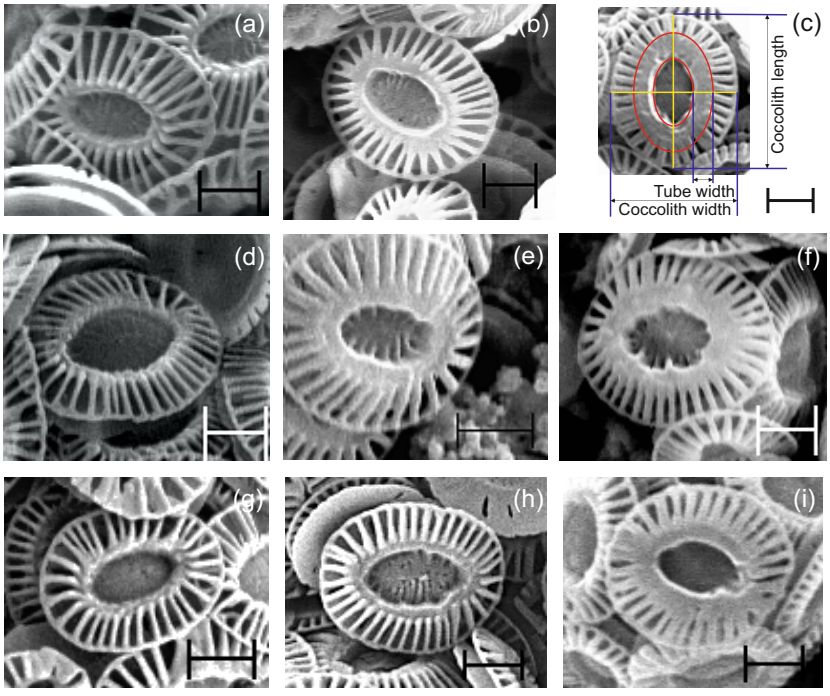

Figure 2. Examples of tube width variations observed in *E. huxleyi* RCC1710 **(a–c)**, RCC1252 **(d–f)**, and IAN01 **(g–i)** coccoliths. Tube width **(c)** was measured along the two semi-minor axes (along the coccolith width) of each coccolith and averaged. Scale bar equal to 1 µm.

2.5 Coccolith length and mass – by polarized light microscopy

Between 10 and 30 mL of culture was filtered with ~ 200 mbar onto cellulose nitrate filters (0.2 µm pore size) and dried at 60 °C for 24 h. A radial piece of filter was embedded and made transparent in immersion oil on microscope slides (e.g. Ziveri et al., 1995).

Images were taken at a magnification of 1000× with a Leica DM6000B cross-polarized light microscope (LM) equipped with a SPOT Insight camera (e.g. Bach et al., 2012; Horigome et al., 2014). Between 50 and 200 image frames from each sample were taken along radial transects and analysed using SYRACO software (Dollfus and Beaufort, 1999; Beaufort and Dollfus, 2004). A minimum of 300 coccolith images were automatically identified by the software and measured in pixels. The software also automatically measures the grey level for each pixel by a birefringence method based on the coccolith brightness when viewed in cross-polarized light (Beaufort, 2005). Coccolith length and mass were subsequently calculated from the pixels and from the measured grey level, respectively, following Horigome et al.

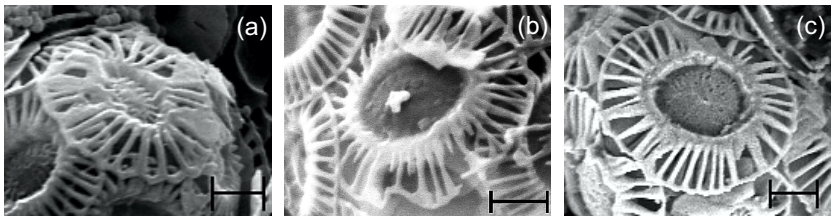

Figure 3. Examples of malformed coccoliths found in *E. huxleyi* RCC1710 **(a)**, RCC1252 **(b)**, and IAN01 **(c)**. Scale bar equal to 1 µm.

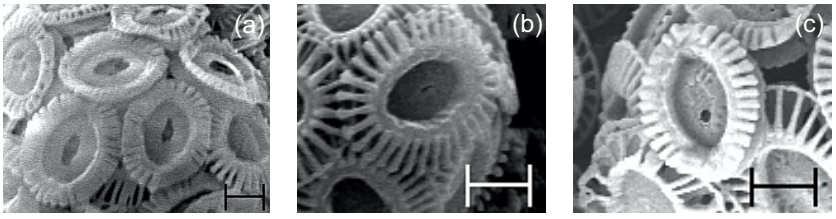

Figure 4. Examples of incomplete coccoliths of *E. huxleyi* RCC1710 **(a)**, RCC1252 **(b)**, and IAN01 **(c)**. Scale bar equal to 1 µm.

(2014) and Beaufort (2005). Therefore, coccolith length was converted from pixels to micrometres, where 832 pixels correspond to 125 µm, and coccolith mass was converted from grey level units to picograms, where 2275.14 grey level units were equivalent to 1 pg of calcite.

2.6 Statistics

For the three *E. huxleyi* strains together, ANOVA (two-factor with replication) was used to test whether a response variable (i.e. growth rate, element variables, morphological variables and mass) presented significant ($p < 0.05$) differences between the temperature treatments, to test whether the effect was strain-independent or strain-specific ($p < 0.05$), and to test whether there were significant differences in the interaction between treatment and strain ($p < 0.05$) and therefore whether the different strains respond similarly or not regardless of whether they were presenting differences between them. If the temperature effect was strain-specific, further ANOVA was used for pairs of strains.

If a response variable presented significant differences between the temperature treatments, and the variable also presented a significant strain-independent response to temperature, or at least the same response on two of the strains, the variable for the similar strains was analysed with simple and multiple linear regressions, including CO_2 partial pressure (pCO_2), CO_3^{2-} concentration and pH, in order to find the useful coefficients (t statistics, $p < 0.05$) of the significant equation (F test, $p < 0.05$) that would estimate the assessed variable value, e.g. the single or combined variables significantly estimating growth rate.

3 Results

3.1 Population growth

The three strains of *E. huxleyi* presented a stable growth rate (per day) that changed with temperature (Fig. 1a, Table 1), with significant differences between the temperature treatments ($F = 244.11$, $p = 0.000$). The strains RCC1710 and RCC1252 presented similar growth rates, not statistically different from one another ($F = 0.372$, $p = 0.550$). From 15 to 25 °C, the IAN01 growth rate was significantly different from the other two *E. huxleyi* strains ($F = 4.53$, $p = 0.025$), but there was no significant difference in the interaction between treatment and strain ($F = 0.71$, $p = 0.597$), so the three strains behaved significantly similarly. The optimum temperature for the three strains was 25 °C. When RCC1710 and RCC1252 were analysed together, changes in growth rate only depended significantly on temperature (linear regression: $R^2 = 0.91$, $F = 229.58$, $p = 0.000$); the carbonate system variables (Table 2) did not much increase the coefficient of determination (maximum to an $R^2 = 0.92$) and none of them were significantly useful in predicting growth rate when used together with temperature (t statistics: $p > 0.05$). According to Eq. (1), on the three strains, a minimum of one duplication per day was obtained from 15 to 27.5 °C.

3.2 Element measurements, ratios and production

Cellular PIC (and its concomitant calcite), POC and TPN (pg cell^{-1}) did not show a consistent trend related to temperature when comparing the three strains of *E. huxleyi* (Fig. 1b, e, h; Table 1). When cellular PIC and TPN response to temperature (from 15 to 25 °C) were statistically analysed (ANOVA), significant differences were found between treatments ($F = 113.42$, $p = 0.000$ and $F = 36.52$, $p = 0.000$,

Table 3. Morphological categorization of coccoliths (from SEM images) of *E. huxleyi* used in this study.

Morphological category	Description
Normal	Regular coccolith in shape, with well-formed distal shield elements aligned forming a symmetric rim. Considered normal when zero or only two malformations were present.
Malformed	Irregular coccolith in shape or size of individual elements and a general reduction in the degree of radial symmetry shown; teratological malformation (Young and Westbroek, 1991). Considered malformed when three or more malformations were present in the coccolith.
Incomplete	Coccolith with variations in its degree of completion according to its normal growing order, with no malformations. Primary calcification variation (Young, 1994).

respectively), but these were not strain-independent ($F = 182.86$, $p = 0.000$ and $F = 33.32$, $p = 0.000$, respectively). Cellular POC, conversely, did not show significant differences between strains ($F = 1.71$, $p = 0.209$), nor did between the temperature treatments ($F = 0.09$, $p = 0.908$). There was no consistent explanatory variable for cellular PIC, POC, and TPN when analysing the three strains independently.

In the three strains, production of PIC (and its concomitant calcite), POC and TPN (pg cell^{-1} day^{-1}) showed a positive relationship with temperature (Fig. 1c, f, i; Table 1). Highest PIC and POC production was in general reached at 25 °C, except for RCC1710, which reached it at 20 °C. From the statistical analysis, PIC and POC production response to temperature, when comparing the three strains of *E. huxleyi* together, was significantly different between the temperature treatments ($F = 8.36$, $p = 0.003$) and the response was strain-independent ($F = 0.89$, $p = 0.428$). Highest TPN production was in general reached at 20 °C, except for RCC1252, which reached it at 25 °C. The latest was supported statistically, as TPN production response, with significant differences between temperature treatments ($F = 499.96$, $p = 0.000$), was strain-specific ($F = 65.92$, $p = 0.000$) when comparing the three strains of *E. huxleyi* together, and yet still the strains RCC1710 and IAN01 presented a similar interaction between treatment and strain ($F = 3.52$, $p = 0.062$); thus, the two strains had a similar behaviour in the TPN production response despite the different values between the strains ($F = 19.02$, $p = 0.000$).

Changes in PIC production on the three strains of *E. huxleyi* mostly depended on temperature (linear regression: $R^2 = 0.89$, $F = 217.36$, $p = 0.000$); pCO_2 with $[CO_3^{2-}]$, when used together with temperature, only slightly increased the coefficient of determination ($R^2 = 0.93$). Changes in POC production on the three strains of *E. huxleyi* only depended significantly on temperature (linear regression: $R^2 = 0.85$, $F = 157.71$, $p = 0.000$).

The PIC : POC ratio decreased from 10 to 20 °C in the three strains of *E. huxleyi* (Fig. 1d). POC was higher than PIC only in the strains RCC1710 and IAN01 at 20 °C. From the statistical analyses, the only significant similitude obtained was in the interaction between treatment and strain for RCC1252 and IAN01 ($F = 2.12$, $p = 0.163$), which means that the PIC : POC ratio behaves similarly towards temperature in these two strains.

The POC : TPN ratio (Fig. 1h) relationship with temperature was strain-specific ($F = 9.59$, $p = 0.001$). The differences between the temperature treatments were significant ($F = 16.95$, $p = 0.000$). There were no significant differences between the strains RCC1710 and RCC1252 ($F = 2.71$, $p = 0.119$), in which the lowest POC : TPN ratio was found at 10 °C; however, there were significant differences in the interaction between treatment and strain ($F = 3.52$, $p = 0.039$), as observed in the different temperatures at which maximum POC : TPN ratios were found for each strain (20 and 25 °C, respectively). The strain IAN01 showed a much different relationship with temperature, with a minimum POC : TPN ratio found at 20 °C.

3.3 Coccolith morphology and mass

Although there was great variation between replicates, mean tube width of coccoliths (Fig. 5a, Table 4) presented a positive trend with temperature, independent of the strain of *E. huxleyi* ($F = 1.73$, $p = 0.204$). Changes in tube width on the three strains of *E. huxleyi* only depended on temperature (linear regression: $R^2 = 0.47$, $F = 28.09$, $p = 0.000$); pCO_2 and $[CO_3^{2-}]$ did not much increase the coefficient of determination ($R^2 = 0.51$) and none of them were significantly useful in predicting tube width when used together with temperature (t statistics: $p > 0.05$).

Coccolith length (Fig. 5b, Table 4) showed a positive trend with temperature, especially on strains RCC1252 and IAN01. The positive trend in strain RCC1710 was not so clear; however, minimum length was also found at 10 °C and maximum length also at 25 °C. Strains RCC1252 and IAN01 were analysed together in a multiple linear regression analysis, as they did not present significant differences

Table 4. Coccoliths morphology and mass. Standard deviation of the triplicates is shown in parentheses.

Strain	T (°C)	Tube width (µm)	Coccolith length (µm)	Coccolith mass (pg)	Malformed (%)	Incomplete (%)
RCC1710	10	0.20 (0.02)	2.03 (0.06)	0.99 (0.11)	33.18 (2.02)	2.39 (0.75)
RCC1710	15	0.22 (0.03)	2.12 (0.03)	1.63 (0.25)	29.19 (4.50)	2.38 (2.36)
RCC1710	20	0.26 (0.02)	2.05 (0.04)	1.75 (0.09)	33.66 (5.85)	8.60 (4.51)
RCC1710	25	0.28 (0.02)	2.16 (0.05)	2.48 (0.16)	37.75 (7.90)	20.10 (5.24)
RCC1252	10	0.21 (0.04)	2.06 (0.00)	1.61 (0.00)	56.39 (3.54)	1.22 (0.51)
RCC1252	15	0.26 (0.05)	2.15 (0.09)	1.97 (0.07)	7.65 (5.29)	1.28 (1.25)
RCC1252	20	0.28 (0.04)	2.27 (0.03)	2.49 (0.30)	10.09 (3.21)	7.09 (5.01)
RCC1252	25	0.27 (0.02)	2.30 (0.03)	3.00 (0.18)	9.09 (3.67)	5.08 (4.85)
IAN01	15	0.22 (0.03)	2.15 (0.06)	2.02 (0.19)	52.13 (8.41)	2.58 (0.66)
IAN01	20	0.25 (0.03)	2.24 (0.00)	2.63 (0.00)	47.09 (2.92)	3.05 (1.78)
IAN01	25	0.27 (0.02)	2.26 (0.02)	2.66 (0.27)	41.18 (4.01)	8.95 (3.01)

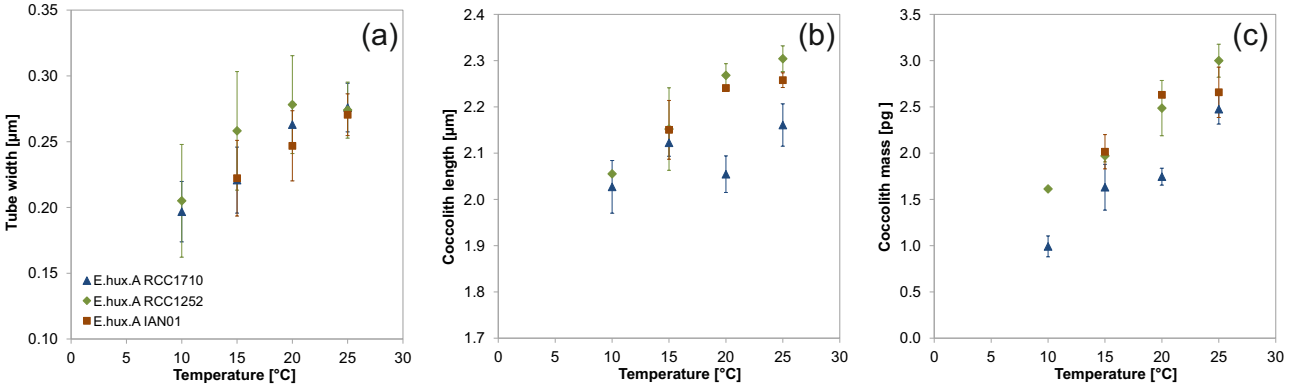

Figure 5. Changes in coccolith morphometry **(a, b)** and mass **(c)**, at different temperatures. Standard deviations of the triplicate experiment results are shown. Three different strains of *E. huxleyi* were used.

between them ($F = 2.12$, $p = 0.171$); temperature gave the highest coefficient of determination ($R^2 = 0.62$, $F = 24.03$, $p = 0.000$) and was the only useful coefficient in estimating coccolith length when making any combination with pCO_2, $[CO_3^{2-}]$ or pH. The strain RCC1710 was analysed independently of the other two strains: temperature presented a low and non-significant coefficient of determination ($R^2 = 0.28$, $F = 3.55$, $p = 0.092$); instead, pH presented the highest coefficient of determination ($R^2 = 0.65$, $F = 16.87$, $p = 0.002$).

The positive relationship of the mean tube width with temperature reflects the increased coccolith calcite quota at higher temperature. Coccolith mass and coccolith size are positively correlated. Why coccolith mass or size should increase with temperature cannot be decisively answered based on our data.

Regardless of the strain, coccolith calcite mass (Fig. 5c, Table 4) showed a positive trend with temperature; significant differences were found between treatments ($F = 35.59$, $p = 0.000$) and no significant differences were found in the interaction between treatment and strain ($F = 2.53$, $p = 0.08$). The strains RCC1252 and IAN01 were analysed together as they did not show significant differences between them ($F = 0.65$, $p = 0.425$). Temperature presented the highest coefficient of determination for RCC1252 and IAN01 ($R^2 = 0.75$, $F = 45.93$, $p = 0.000$) and also for RCC1710 ($R^2 = 0.87$, $F = 58.58$, $p = 0.000$), and adding other coefficients was not significantly useful in estimating coccolith mass. On average, coccolith mass increased with temperature $\sim 2.2\times$ from 10 to 25 °C, $\sim 1.5\times$ from 15 to 25 °C, and $\sim 1.2\times$ from 20 to 25 °C; on average, coccolith mass increased $1.28\times$ (or 0.45 pg) each 5 °C.

The percentage of malformed coccoliths per sample (Fig. 6a, Table 4) did not show a consistent trend with temperature when comparing the three strains of *E. huxleyi* ($F = 113.21$, $p = 0.000$). Only one strain (RCC1252) presented significant differences between the temperature treatments, with higher percentage at the lowest experimented temperature.

Only in strain RCC1710, the percentage of incomplete coccoliths presented a significant increase with temperature (Fig. 6b, Table 4). Higher percentages of incomplete coccol-

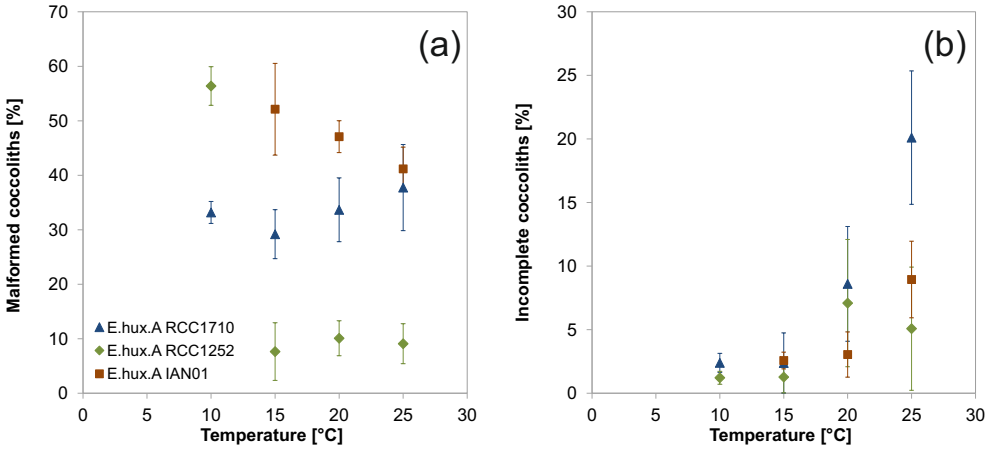

Figure 6. Percentage of malformed **(a)** and incomplete **(b)** coccoliths in three *E. huxleyi* strains grown at different temperatures. Standard deviations of the triplicate experiment results are shown.

iths in strain RCC1710 were found at 25 °C. ANOVA results showed that, between the three strains, there were no significant differences between only the strains RCC1252 and IAN01 ($F = 0.06$, $p = 0.810$) and their interaction between treatment and strain ($F = 2.33$, $p = 0.139$), though in this case (analysed from 15 to 25 °C) there were also no significant differences between the temperature treatments ($F = 3.78$, $p = 0.053$). Significant strain-independent and strain-specific responses of *E. huxleyi* to temperature, found in the three strains of this study, are summarized in Table 5.

4 Discussion

4.1 Growth rate, elemental production and incomplete coccoliths

All three *E. huxleyi* strains investigated here displayed similar growth rate versus temperature relationships, with an optimum at 20–25 °C (Fig. 1a). This is a typical range for many *E. huxleyi* strains (e.g. Watabe and Wilbur, 1966; Van Rijssel and Gieskes, 2002; Sorrosa et al., 2005; De Bodt et al., 2010; Langer et al., 2009). We expect that strains isolated, for example, in the Arctic will have a lower temperature optimum, though. Also not untypical, elemental production (PIC, POC, TPN) increased with temperature over the sub-optimum to optimum temperature range (Fig. 1; Langer et al., 2007; Sett et al., 2014). It is intuitive that, approaching optimum, higher temperature increases elemental production, because biochemical rates are temperature-dependent. It is also intuitive that the percentage of incomplete coccoliths should increase with higher P_{PIC}, as indeed observed in RCC1710 (Fig. 6b). The idea underlying this intuition is that less time is taken to produce one coccolith and that the production process is stopped before the coccolith is fully formed. A comparison of RCC1710 and RCC1252 shows how wrong this idea is (Table 6). The percentage of incomplete coccoliths increases in the former only. While it is true that coccolith production time in RCC1710 decreases from 31 min at 10 °C to 22 min at 25 °C, this decrease is even more pronounced in RCC1252 (from 88 to 23 min). Hence, RCC1252 should show a steeper increase in incompleteness than RCC1710. This is not the case. Please note that the increase in incompleteness in RCC1252 (Fig. 6b) is not significant, because the increase is well below 10 % and the error bars overlap (see also Langer et al., 2013, for a discussion of this criterion). Another piece of evidence which does not fit the "premature release of coccoliths because of time shortage" idea is that both RCC1710 and RCC1252 manage to produce heavier coccoliths in a shorter time at higher temperature (Tables 4 and 6). We do not know why the stop signal for coccolith growth is affected by temperature in RCC1710. Nothing is known about the biochemical underpinning of that stop signal, so it is unfortunately impossible to speculate about the mechanism of a temperature effect. It was, however, argued that the processes involved in the stop signal are different from those producing teratological malformations (Young and Westbroek, 1991; Langer et al., 2010, 2011). This is supported by our data, because there is no correlation between incompleteness and malformations (Fig. 6). We will discuss malformations in Sect. 4.3.

Interestingly coccolith mass is positively correlated with temperature (and P_{PIC}) in all strains tested here. The positive correlation of coccolith mass and P_{PIC} was also observed by Bach et al. (2012) in a carbonate chemistry manipulation experiment and is the basis of using coccolith mass as a proxy for P_{PIC} (Beaufort et al., 2011). This is an interesting option, because in field samples coccolith mass might be a promising indicator of P_{PIC}. There are only few proxies available to reconstruct past coccolithophore P_{PIC}, the traditional one being the calcite Sr / Ca ratio, established at the turn of the millennium (Stoll and Schrag, 2000). Analysing Sr / Ca, how-

Table 5. Significant strain-independent and strain-specific responses of *E. huxleyi* to temperature found in the three strains of this study.

Strain-independent responses	Strain-specific responses
– Growth rate optimum temperature was 25 °C. – Highest PIC, POC, and TPN production values were found at 20 or 25 °C. – The PIC : POC ratio decreased from 10 to 20 °C. – Tube width increased with temperature, from ∼ 0.20 µm at 10 °C to ∼ 0.27 µm at 25 °C. – Maximum coccolith length was found at 25 °C. – Coccolith mass increased with temperature (∼ 2.2× from 10 to 25 °C, ∼ 1.5× from 15 to 25 °C, and ∼ 1.2× from 20 to 25 °C; on average, 0.45 pg each 5 °C).	– Cellular PIC, POC and TPN (pg per cell). – POC : TPN ratio. However, in the two strains tested at 10 °C (RCC1710 and RCC1252), the POC : TPN ratio was lowest at 10 °C. – Percentage of malformed coccoliths per sample. – Percentages of incomplete coccoliths. – Coccolith length, although in strains RCC1252 and IAN01 was positively correlated with temperature.

Table 6. Coccolith production time. Standard deviation of the triplicates is shown in parentheses. Lith: coccolith; d: day; h: hour; min: minutes.

Strain	T (°C)	pg PIC lith^{-1}	lith cell^{-1}	lith cell^{-1} d^{-1}	lith cell^{-1} h^{-1}	min lith^{-1}	pg PIC h^{-1}
RCC1710	10	0.12 (0.01)	121 (2)	31 (0)	2.0 (0.0)	31 (0)	0.25 (0.00)
RCC1710	15	0.20 (0.03)	74 (14)	55 (10)	3.4 (0.6)	18 (3)	0.66 (0.03)
RCC1710	20	0.21 (0.01)	53 (0)	61 (1)	3.8 (0.1)	16 (0)	0.82 (0.01)
RCC1710	25	0.30 (0.02)	36 (2)	45 (2)	2.8 (0.1)	22 (1)	0.83 (0.03)
RCC1252	10	0.19 (0.00)	43 (2)	11 (2)	0.7 (0.1)	88 (18)	0.13 (0.02)
RCC1252	15	0.24 (0.01)	42 (1)	31 (1)	1.9 (0.1)	31 (1)	0.45 (0.01)
RCC1252	20	0.30 (0.04)	35 (6)	42 (4)	2.6 (0.2)	23 (2)	0.75 (0.05)
RCC1252	25	0.36 (0.02)	34 (3)	41 (3)	2.6 (0.2)	23 (2)	0.93 (0.02)
IAN01	15	0.24 (0.02)	42 (3)	34 (2)	2.1 (0.2)	28 (2)	0.51 (0.01)
IAN01	20	0.32 (0.00)	26 (1)	30 (1)	1.9 (0.0)	32 (1)	0.59 (0.02)
IAN01	25	0.32 (0.03)	35 (5)	47 (6)	2.9 (0.4)	21 (3)	0.93 (0.03)

ever, requires either a sizable sample or comparatively sophisticated secondary ion mass spectrometry (SIMS) measurements (Stoll et al., 2007; Prentice et al., 2014). Recently, coccosphere diameter and coccolith quota were introduced as growth rate proxies (Gibbs et al., 2013). However, complete coccospheres are the exception rather than the rule in sediment samples, so it is important to have a proxy based on individual coccoliths. Hence, coccolith mass and size (which are correlated; Fig. 5, Table 4) are an option which it is worthwhile exploring in the future.

4.2 *Emiliania huxleyi* PIC : POC response

As detailed in the introduction there is considerable variability in the PIC : POC response of *E. huxleyi* to temperature changes. This variability cannot be traced back to strain-specific features, but it might partly reflect the fact that different temperature ranges were investigated, mostly without the knowledge of the optimum temperature. Other experimental conditions, such as light intensity and nutrient concentrations, varied and might have also played a role (Hoppe et al., 2011). In this study we ran three strains under identical conditions and, for the first time, are presented with a coherent picture. All three strains display a bell-shaped curve with lowest PIC : POC close to the optimum growth temperature (Fig. 1d). Although our data on the right-hand side of the PIC : POC minimum are not conclusive for RCC1252, the bell-shaped curve is discernible in the latter strain. This finding seems to fit data on other *E. huxleyi* strains (De Bodt et al., 2010; Sett et al., 2014) and on *C. pelagicus* (Gerecht et al., 2014). This comparison is, however, not straightforward since two of the studies (De Bodt et al., 2010; Gerecht et al., 2014) employed two temperatures, one of the studies employed three temperatures (Sett et al., 2014), only without determining the optimum temperature in all three studies. Be that as it may, based on our data, we might conclude that *E. huxleyi* tends to show the lowest PIC : POC close to its optimum growth temperature. In the context of global warming, that would mean that, in the future, *E. huxleyi* and possibly coccolithophore PIC : POC will tend to decrease because most strains live at sub-optimal temperatures in the field (Buitenhuis et al., 2008; Langer et al., 2009; Heinle, 2014). This trend might be pronounced because global warming is accompanied by lower surface water nutrient levels and ocean acidification (Cermeño et al., 2008; Doney et al., 2009). All these changes apparently cause a decrease in *E. huxleyi*'s PIC : POC (our data; Hoppe et al., 2011; Oviedo et al., 2014). A marked decline in coccolithophore PIC : POC will have implications for long-term carbon burial and might even affect surface water carbonate chemistry on

short timescales, i.e. 1 year (Barker et al., 2003; Ridgwell and Zeebe, 2005; Cermeño et al., 2008).

4.3 Coccolith malformations

The coccolith shaping machinery is, besides the ion transport machinery, an essential part of coccolith formation (for an overview see Holtz et al., 2013). The latter commences with heterogeneous nucleation on an organic template, the so-called base plate. The nucleation determines crystal axis orientation. Crystal growth proceeds in principle inorganically, with the notable exception that crystal shape is strongly modified by means of a dynamic mould, which essentially consists in the coccolith vesicle shaped by cytoskeleton elements and polysaccharides inside the coccolith vesicle. Malformations can be due to an abnormal base plate which would affect crystal axis orientation, aberrations in the composition or structure of the polysaccharides, and disturbance of cytoskeleton functionality. The last of these would most likely also cause a decline in growth rate, which is why this mechanism was disregarded in the case of carbonate-chemistry-induced malformations (Langer et al., 2011). By the same reasoning, temperature-induced malformations might be due to cytoskeleton disturbance, because temperature does also alter growth rate (Fig. 1a). However, it is not straightforward to see why lower than optimum temperature should disturb cytoskeleton functionality (see also Langer et al., 2010). At any rate, coccolith malformations are most likely detrimental to fitness, because malformed coccoliths result in fragile coccospheres, which are regarded as instrumental in coccolithophore fitness (Dixon, 1900; Young, 1994; Langer and Bode, 2011; Langer et al., 2011). One of the many hypotheses concerning function of calcification is that the coccosphere confers mechanical protection (Dixon, 1900; Young, 1994). After more than a century of research, it still remains the most plausible hypothesis.

Coccolith malformations, i.e. disturbances of the coccolith shaping machinery, occur in both field and culture samples, but usually more so in the latter (Langer et al., 2006, 2013). The causes of malformations are only partly known. In cultured samples, artificial conditions (not present in the field) such as cell densities of 10^6 cells mL^{-1}, cells sitting on the bottom of the culture flask, stagnant water, and confinement in a culture flask play a role in inducing the surplus of malformations compared to field samples (Langer et al., 2013; Ziveri et al., 2014). However, in the field malformations do occur, and sometimes in considerable percentages (Giraudeau et al., 1993; Ziveri et al., 2014). The environmental conditions leading to elevated levels of malformations have long since been disputed. Besides nutrient limitation (Honjo, 1976), temperature and carbonate chemistry are conspicuous candidates. Although the range of temperatures used here exceeds 2100 projections (IPCC, 2013), we used it not only on physiological grounds but also for ecological reasons. Over the course of the year, coccolithophores in the North Pacific experience the whole range of temperatures used here (http://disc.sci.gsfc.nasa.gov/giovanni/, maps in the Supplement). In a seminal experimental study it was shown that moving away from the optimal growth temperature increases malformations in *E. huxleyi* (Watabe and Wilbur, 1966). This result was confirmed for higher than optimum temperature in another strain (Langer et al., 2010) but could not be confirmed for sub-optimal temperature in two strains (De Bodt et al., 2010; Langer et al., 2010). The sub-optimal temperature range is of particular interest because most clones live at sub-optimal temperatures in the field. Here we investigated sub-optimum to optimum temperatures in three further strains. While RCC1710 showed no change in the percentage of malformations and IAN01 featured a shallow gradual increase from 25 to 15 °C, RCC1252 was insensitive over the latter range but displayed a steep increase in malformations at 10 °C (Fig. 6). Based on our own and the literature data, we conclude that the sub-optimal temperature effect on morphogenesis is strain-specific. The fact that the base level of malformations in cultured coccolithophores differs between species and strains (and also varies with time) has been recognized for many years and is now well documented (e.g. Langer and Benner, 2009; Langer et al., 2011, 2013). Also, the response of the morphogenetic machinery to environmental factors is strain-specific (Langer et al., 2011). We currently do not have enough accessory information to formulate a hypothesis why exactly one strain differs from another. The fact that they do indeed differ, however, probably reflects the high genetic diversity in *E. huxleyi*.

Can we see a pattern in this strain specificity? It is intriguing that *E. huxleyi* clones fall into two distinct groups characterized by their temperature preference: the warm-water and the cool-water group (Hagino et al., 2011). Of the strains analysed for morphology, the following belong to the warm-water group: BT-6 (Watabe and Wilbur, 1966), RCC1710, RCC1252, and possibly RCC1238 (Langer et al., 2010). The latter was unfortunately not included in the study by Hagino et al. (2011). Since these strains display different responses to temperature, their being part of the warm-water group does unfortunately not help finding common features of sensitive strains. However, only a few strains have been studied so far, and it might be worthwhile testing a statistical number from the warm-water and the cool-water group.

5 Conclusions

1. Temperature, PIC production, coccolith mass, and coccolith size are positively correlated. Since the positive correlation between coccolith mass and PIC production was observed in response to seawater carbonate chemistry changes as well (Bach et al., 2012), it can be hypothesized that coccolith mass might be a good proxy for PIC production independent of the environmental parameter causing the change in PIC production.

2. Sub-optimal growth temperature was identified as one of the potential causes of coccolith malformations in the field. Since the effect of sub-optimal temperature on coccolith morphogenesis is strain-specific, a statistically relevant number of strains have to be tested in order to clarify whether this effect is indeed ecologically relevant.

3. We consistently showed for the first time that *E. huxleyi* features a PIC : POC minimum under optimum growth temperature. Taken together with literature data, this finding suggests that global environmental change will lead to a marked decrease in PIC : POC of *E. huxleyi* and possibly coccolithophores as a group.

The Supplement related to this article is available online at doi:10.5194/bg-13-2913-2016-supplement.

Acknowledgements. This work was funded by the European Union's Seventh Framework Programme under grant agreement 265103 (project MedSeA), the European Research Council (ERC grant 2010-NEWLOG ADG-267931 HE), the Generalitat de Catalunya (MERS, 2014 SGR – 1356) and the Natural Environment Research Council (NE/N011708/1). Anaid Rosas-Navarro also acknowledges the "MECD/SGU/DGPU, Programa Estatal de Promoción del Talento y su Empleabilidad" (Becas FPU) of the MINECO, Spain; thanks the technical and personal support from researchers and technicians at the Alfred Wegener Institute for Polar and Marine Research (AWI), where the laboratory experiments were done; thanks Michael Grelaud for his advice on the use of the software SYRACO; and thanks Yannick A. de Icaza A. for his scientific feedback and financial support. We thank the referees for the constructive comments that greatly helped to improve the manuscript. This work is contributing to the ICTA "Unit of Excellence" (MinECo, MDM2015-0552).

Edited by: H. Kitazato

References

Bach, L. T., Bauke, C., Meier, K. J. S., Riebesell, U., and Schulz, K. G.: Influence of changing carbonate chemistry on morphology and weight of coccoliths formed by *Emiliania huxleyi*, Biogeosciences, 9, 3449–3463, doi:10.5194/bg-9-3449-2012, 2012.

Barker, S., Higgins, J. A., and Elderfield, H.: The future of the carbon cycle: review, calcification response, ballast and feedback on atmospheric CO_2, Philos. T. R. Soc. A, 361, 1977–1999, 2003.

Beaufort, L.: Weight estimates of coccoliths using the optical properties (birefringence) of calcite, Micropaleontology, 51, 289–297, 2005.

Beaufort, L. and Dollfus, D.: Automatic recognition of coccoliths by dynamical neural networks, Mar. Micropaleontol., 51, 57–73, 2004.

Beaufort, L., Probert, I., de Garidel-Thoron, T., Bendif, E. M., Ruiz-Pino, D., Metzl, N., Goyet, C., Buchet, N., Coupel, P., Grelaud, M., Rost, B., Rickaby, R. E. M., and de Vargas, C.: Sensitivity of coccolithophores to carbonate chemistry and ocean acidification, Nature, 476, 80–83, 2011.

Bollmann, J.: Morphology and biogeography of Gephyrocapsa coccoliths in Holocene sediments, Mar. Micropaleontol., 29, 319–350, 1997.

Bradshaw, A. L., Brewer, P. G., Shafer, D. K., and Williams, R. T.: Measurements of total carbon dioxide and alkalinity by potentiometric titration in the GEOSECS program, Earth Planet. Sc. Lett., 55, 99–115, 1981.

Brewer, P., Bradshaw, A., and Williams, R.: Measurements of Total Carbon Dioxide and Alkalinity in the North Atlantic Ocean in 1981, in: The Changing Carbon Cycle, edited by: Trabalka, J. and Reichle, D., Springer New York, 348–370, 1986.

Brown, C.: Global Distribution of Coccolithophore Blooms, Oceanography, 8, 59–60, 1995.

Brownlee, C. and Taylor, A.: Calcification in coccolithophores : A cellular perspective, in: Coccolithophores: from molecular processes to global impacts, edited by: Young, J. R. and Thierstein, H. R., Springer Berlin Heidelberg, Berlin, Heidelberg, 31–49, 2004.

Buitenhuis, E., Van Bleijswijk, J., Bakker, D., and Veldhuis, M.: Trends in inorganic and organic carbon in a bloom of *Emiliania huxleyi* in the North Sea, Mari. Ecol. Prog. Serie., 143, 271–282, 1996.

Buitenhuis, E. T., Pangerc, T., Franklin, D. J., Le Quéré, C., and Malin, G.: Growth rates of six coccolithophorid strains as a function of temperature, Limnol. Oceanogr., 53, 1181–1185, 2008.

Cermeño, P., Dutkiewicz, S., Harris, R. P., Follows, M., Schofield, O., and Falkowski, P. G.: The role of nutricline depth in regulating the ocean carbon cycle, Proc. Natl. Acad. Sci., 105, 20344–20349, 2008.

Cubillos, J. C., Wright, S. W., Nash, G., de Salas, M. F., Griffiths, B., Tilbrook, B., Poisson, A., and Hallegraeff, G. M.: Calcification morphotypes of the coccolithophorid *Emiliania huxleyi* in the Southern Ocean: changes in 2001 to 2006 compared to historical data, Mar. Ecol. Prog. Serie., 348, 47–54, 2007.

De Bodt, C., Van Oostende, N., Harlay, J., Sabbe, K., and Chou, L.: Individual and interacting effects of pCO_2 and temperature on *Emiliania huxleyi* calcification: study of the calcite production, the coccolith morphology and the coccosphere size, Biogeosciences, 7, 1401–1412, doi:10.5194/bg-7-1401-2010, 2010.

Dickson, A. and Millero, F.: A comparison of the equilibrium constants for the dissociation of carbonic acid in seawater media, Deep-Sea Res. Pt. A, 34, 1733–1743, 1987.

Dixon, H. H.: On the Structure of Coccospheres and the Origin of Coccoliths, Proc. Roy. Soc. Lond., 66, 305–315, 1900.

Dollfus, D. and Beaufort, L.: Fat neural network for recognition of position-normalised objects, Neural Networks, 12, 553–560, 1999.

Doney, S. C., Fabry, V. J., Feely, R. A., and Kleypas, J. A.: Ocean acidification: the other CO_2 problem, Ann. Rev. Mar. Sci., 1, 169–92, 2009.

Feng, Y., Warner, M. E., Zhan, Y., Sun, J., Fu, F., Rose, J. M., and Hutchins, D. A.: Interactive effects of increased pCO_2, temperature and irradiance on the marine coccolithophore *Emiliania huxleyi* (Prymnesiophyceae), Eur. J. Phycol., 43, 87–98, 2008.

Findlay, H. S., Calosi, P., and Crawfurd, K.: Determinants of the PIC : POC response in the coccolithophore *Emiliania huxleyi* under future ocean acidification scenarios, Limnol. Oceanogr., 56, 1168–1178, 2011.

Gerecht, A. C., Šupraha, L., Edvardsen, B., Probert, I., and Henderiks, J.: High temperature decreases the PIC / POC ratio and increases phosphorus requirements in *Coccolithus pelagicus* (Haptophyta), Biogeosciences, 11, 3531–3545, doi:10.5194/bg-11-3531-2014, 2014.

Gibbs, S. J., Poulton, A. J., Bown, P. R., Daniels, C. J., Hopkins, J., Young, J. R., Jones, H. L., Thiemann, G. J., O'Dea, S. A., and Newsam, C.: Species-specific growth response of coccolithophores to Palaeocene-Eocene environmental change, Nat. Geosci., 6, 218–222, 2013.

Giraudeau, J., Monteiro, P. M., and Nikodemus, K.: Distribution and malformation of living coccolithophores in the northern Benguela upwelling system off Namibia, Mar. Micropaleontol., 22, 93–110, 1993.

Gran, G.: Determination of the equivalence point in potentiometric titrations of seawater with hydrochloric acid, Oceanol. Acta, 5, 209–218, 1952.

Guillard, R. R. and Ryther, J. H.: Studies of marine planktonic diatoms. I. Cyclotella nana Hustedt, and Detonula confervacea (cleve) Gran, Can. J. Microbiol., 8, 229–239, 1962.

Hagino, K. and Okada, H.: Intra- and infra-specific morphological variation in selected coccolithophore species in the equatorial and subequatorial Pacific Ocean, Mar. Micropaleontol., 58, 184–206, 2006.

Hagino, K., Okada, H., and Matsuoka, H.: Coccolithophore assemblages and morphotypes of *Emiliania huxleyi* in the boundary zone between the cold Oyashio and warm Kuroshio currents off the coast of Japan, Mar. Micropaleontol., 55, 19–47, 2005.

Hagino, K., Bendif, E. M., Young, J. R., Kogame, K., Probert, I., Takano, Y., Horiguchi, T., de Vargas, C., and Okada, H.: New evidence for morphological and genetic variation in the cosmopolitan coccolithophore *Emiliania huxleyi* (Prymnesiophyceae) from the COX1b-ATP4 GENES1, J. Phycol., 47, 1164–1176, 2011.

Harada, N., Sato, M., Oguri, K., Hagino, K., Okazaki, Y., Katsuki, K., Tsuji, Y., Shin, K.-H., Tadai, O., Saitoh, S.-I., Narita, H., Konno, S., Jordan, R. W., Shiraiwa, Y., and Grebmeier, J.: Enhancement of coccolithophorid blooms in the Bering Sea by recent environmental changes, Global Biogeochem. Cy., 26, GB2036, doi:10.1029/2011GB004177, 2012.

Heinle, M.: The effects of light, temperature and nutrients on coccolithophores and implications for biogeochemical models, Ph.D. thesis, University of East Anglia, School of Environmental Sciences, Norwich, UK, https://ueaeprints.uea.ac.uk/48676/1/thesis_Heinle.pdf, 2014.

Holtz, L.-M., Langer, G., Rokitta, S., and Thoms, S.: Green biosynthesis of nanoparticles: mechanisms and applications, chap. Synthesis of nanostructured calcite particles in coccolithophores, unicellular algae, CABI, Wallingford, UK, 132–147, doi:10.1079/9781780642239.0132, 2013.

Honjo, S.: Coccoliths: Production, transportation and sedimentation, Mar. Micropaleontol., 1, 65–79, 1976.

Hoppe, C. J. M., Langer, G., and Rost, B.: *Emiliania huxleyi* shows identical responses to elevated pCO_2 in TA and DIC manipulations, J. Exp. Mar. Biol. Ecol., 406, 54–62, 2011.

Horigome, M. T., Ziveri, P., Grelaud, M., Baumann, K.-H., Marino, G., and Mortyn, P. G.: Environmental controls on the *Emiliania huxleyi* calcite mass, Biogeosciences, 11, 2295–2308, doi:10.5194/bg-11-2295-2014, 2014.

Iglesias-Rodríguez, M. D., Schofield, O. M., Batley, J., Medlin, L. K., and Hayes, P. K.: Intraspecific genetic diversity in the marine coccolithophore *Emiliania huxleyi* (Prymnesiophyceae): The use of microsatellite analysis in marine phytoplankton population studies, J. Phycol., 42, 526–536, 2006.

IPCC: Climate Change 2013: The Physical Science Basis. Contribution of Working Group I to the Fifth Assessment Report of the Intergovernmental Panel on Climate Change, 1535, Cambridge University Press, Cambridge, United Kingdom and New York, NY, USA, 2013.

Langer, G. and Benner, I.: Effect of elevated nitrate concentration on calcification in *Emiliania huxleyi*, Journal of Nannoplankton Research, 30, 77–80, 2009.

Langer, G. and Bode, M.: CO_2 mediation of adverse effects of seawater acidification in *Calcidiscus leptoporus*, Geochem. Geophy. Geosy., 12, q05001, doi:10.1029/2010GC003393, 2011.

Langer, G., Geisen, M., Baumann, K. H., Klas, J., Riebesell, U., Thoms, S., and Young, J. R.: Species-specific responses of calcifying algae to changing seawater carbonate chemistry, Geochem. Geophy. Geosy., 7, Q09006, doi:10.1029/2005GC001227, 2006.

Langer, G., Gussone, N., Nehrke, G., Riebesell, U., Eisenhauer, A., and Thoms, S.: Calcium isotope fractionation during coccolith formation in *Emiliania huxleyi*: Independence of growth and calcification rate, Geochemistry, Geophysics, Geosystems, 8, Q05007, doi:10.1029/2006GC001422, 2007.

Langer, G., Nehrke, G., Probert, I., Ly, J., and Ziveri, P.: Strain-specific responses of *Emiliania huxleyi* to changing seawater carbonate chemistry, Biogeosciences, 6, 2637–2646, doi:10.5194/bg-6-2637-2009, 2009.

Langer, G., De Nooijer, L. J., and Oetjen, K.: On the role of the cytoskeleton in coccolith morphogenesis: The effect of cytoskeleton inhibitors, J. Phycol., 46, 1252–1256, 2010.

Langer, G., Probert, I., Nehrke, G., and Ziveri, P.: The morphological response of *Emiliania huxleyi* to seawater carbonate chemistry changes: an inter-strain comparison, Journal of Nannoplankton Research, 32, 29–34, 2011.

Langer, G., Oetjen, K., and Brenneis, T.: On culture artefacts in coccolith morphology, Helgoland Mar. Res., 67, 359–369, 2013.

Lewis, E. and Wallace, D. W. R.: Program Developed for CO_2 System Calculations ORNL/CDIAC-105, Carbon Dioxide Information Analysis Centre, Oak Ridge National Laboratory, Laboratory, US Department of Energy, 1998.

McIntyre, A. and Bé, A. W.: Modern coccolithophoridae of the atlantic ocean – I. Placoliths and cyrtoliths, 1967.

Medlin, L. K., Barker, G. L. A., Campbell, L., Green, J. C., Hayes, P. K., Marie, D., Wrieden, S., and Vaulot, D.: Genetic characterisation of *Emiliania huxleyi* (Haptophyta), J. Mar. Syst., 9, 13–31, 1996.

Mehrbach, C., Culberson, C. H., Hawley, J. E., and Pytkowicz, R. M.: Measurement of the apparent dissociation constants of carbonic acid in seawater at atmospheric pressure, Limnol. Oceanogr., 18, 897–907, 1973.

Oviedo, A. M., Langer, G., and Ziveri, P.: Effect of phosphorus limitation on coccolith morphology and element ratios in Mediter-

ranean strains of the coccolithophore *Emiliania huxleyi*, J. Exp. Mar. Biol. Ecol., 459, 105–113, 2014.

Paasche, E.: A review of the coccolithophorid *Emiliania huxleyi* (Prymnesiophyceae), with particular reference to growth, coccolith formation, and calcification-photosynthesis interactions, Phycologia, 40, 503–529, 2001.

Prentice, K., Jones, T. D., Lees, J., Young, J., Bown, P., Langer, G., and Fearn, S.: Trace metal (Mg / Ca and Sr / Ca) analyses of single coccoliths by Secondary Ion Mass Spectrometry, Geochim. Cosmochim. Ac., 146, 90–106, 2014.

Read, B. a., Kegel, J., Klute, M. J., Kuo, A., Lefebvre, S. C., Maumus, F., Mayer, C., Miller, J., Monier, A., Salamov, A., Young, J., Aguilar, M., Claverie, J.-M., Frickenhaus, S., Gonzalez, K., Herman, E. K., Lin, Y.-C., Napier, J., Ogata, H., Sarno, A. F., Shmutz, J., Schroeder, D., de Vargas, C., Verret, F., von Dassow, P., Valentin, K., Van de Peer, Y., Wheeler, G., Dacks, J. B., Delwiche, C. F., Dyhrman, S. T., Glöckner, G., John, U., Richards, T., Worden, A. Z., Zhang, X., and Grigoriev, I. V.: Pan genome of the phytoplankton Emiliania underpins its global distribution, Nature, 499, 209–13, 2013.

Ridgwell, A. and Zeebe, R. E.: The role of the global carbonate cycle in the regulation and evolution of the Earth system, Earth Planet. Sc. Lett., 234, 299–315, 2005.

Robertson, J., Robinson, C., Turner, D., Holligan, P., Watson, A., Boyd, P., Fernandez, E., and Finch, M.: The impact of a coccolithophore bloom on oceanic carbon uptake in the northeast Atlantic during summer 1991, Deep-Sea Res. Pt. I, 41, 297–314, 1994.

Schroeder, D. C., Biggi, G. F., Hall, M., Davy, J., Martinez, J. M., Richardson, A. J., Malin, G., and Wilson, W. H.: A genetic marker to separate *Emiliania huxleyi* (Prymnesiophyceae) morphotypes1, J. Phycol., 41, 874–879, 2005.

Sett, S., Bach, L. T., Schulz, K. G., Koch-Klavsen, S., Lebrato, M., and Riebesell, U.: Temperature modulates coccolithophorid sensitivity of growth, photosynthesis and calcification to increasing seawater pCO_2, PloS One, 9, e88308, doi:10.1371/journal.pone.0088308, 2014.

Sorrosa, J. M., Satoh, M., and Shiraiwa, Y.: Low temperature stimulates cell enlargement and intracellular calcification of coccolithophorids, Marine biotechnology (New York, NY), 7, 128–33, 2005.

Stoll, H. M. and Schrag, D. P.: Coccolith Sr / Ca as a new indicator of coccolithophorid calcification and growth rate, Geochem. Geophy. Geosy., 1, 1006, doi:10.1029/1999GC000015, 2000.

Stoll, H. M., Shimizu, N., Archer, D., and Ziveri, P.: Coccolithophore productivity response to greenhouse event of the Paleocene-Eocene Thermal Maximum, Earth Planet. Sc. Lett., 258, 192–206, 2007.

Van Rijssel, M. and Gieskes, W. W. C.: Temperature, light, and the dimethylsulfoniopropionate (DMSP) content of *Emiliania huxleyi* (Prymnesiophyceae), J. Sea Res., 48, 17–27, 2002.

Watabe, N. and Wilbur, K. M.: Effects of temperature on growth, calcification, and coccolith form in *Coccolithus huxleyi* (Coccolithineae), Limnol. Oceanogr., 11, 567–575, 1966.

Westbroek, P., Brown, C. W., van Bleijswijk, J., Brownlee, C., Brummer, G. J., Conte, M., Egge, J., Fernández, E., Jordan, R., Knappertsbusch, M., Stefels, J., Veldhuis, M., van der Wal, P., and Young, J.: A model system approach to biological climate forcing, The example of *Emiliania huxleyi*, Glob. Planet. Change, 8, 27–46, 1993.

Young, J. R.: Variation in *Emiliania huxleyi* coccolith morphology in samples from the Nowegian Ehux experiment, Sarsia, 79, 417–425, 1994.

Young, J. R. and Westbroek, P.: Genotypic variation in the coccolithophorid species *Emiliania huxleyi*, Mar. Micropaleontol., 18, 5–23, 1991.

Ziveri, P., Thunell, R. C., and Rio, D.: Export production of coccolithophores in an upwelling region: Results from San Pedro Basin, Southern California Borderlands, Mar. Micropaleontol., 24, 335–358, 1995.

Ziveri, P., Baumann, K. H., Böckel, B., Bollmann, J., and Young, J. R.: Biogeography of selected Holocene coccoliths in the Atlantic Ocean, in: Coccolithophores: from molecular process to global impact, Springer Berlin Heidelberg, Berlin, Heidelberg, 403–428, 2004.

Ziveri, P., Passaro, M., Incarbona, A., Milazzo, M., Rodolfo-Metalpa, R., and Hall-Spencer, J. M.: Decline in coccolithophore diversity and impact on coccolith morphogenesis along a natural CO_2 gradient, Biol. Bull., 226, 282–290, 2014.